PROCEEDINGS of the
23rd International Congress on Acoustics

9 to 13 September 2019 in Aachen, Germany

Analysis Methods and Design Measures for the Reduction of Noise and Vibration Induced by Marine Propellers

Julian KIMMERL[1]; Paul MERTES[1]; Vladimir KRASILNIKOV[2]; Kourosh KOUSHAN[2]; Luca SAVIO[2]; Mario FELLI[3]; Moustafa ABDEL-MAKSOUD[4]; Ulf GÖTTSCHE[4]; Nils REICHSTEIN[5]

[1] SCHOTTEL GmbH, Mainzer Straße 99, 56322 Spay, Germany

[2] SINTEF Ocean, Otto Nielsens veg 10, 7052 Trondheim, Norway

[3] CNR INM, Via di Vallerano 139, 00128 Rome, Italy

[4] Technical University Hamburg-Harburg, Am Schwarzenberg-Campus 4, 21073 Hamburg, Germany

[5] Fr. Lürssen Werft GmbH & Co. KG, Zum Alten Speicher 11, 28759 Bremen-Vegesack, Germany

ABSTRACT

The paper presents the ongoing work in the research project ProNoVi. The objective of the project is to improve the numerical and experimental methods for the prediction of noise and vibrations induced by a propeller operating behind ship hull in full-scale conditions. Based on the improved methods practical recommendations for the reduction of noise and vibration levels for different classes of vessels are a further objective. The propeller cavitation noise is identified as the dominating noise source, which coincides with important frequencies of perception of marine fauna and thus may have negative impact on marine life. As a side effect, reducing the noise under water will increase comfort and thus safety for crew and passengers on board. The project aims at delivering a better understanding of fundamental physical mechanisms related to turbulence, induced vorticity and cavitation dynamics, which play a decisive role in generation of tonal and broadband propeller noise. The project partners will give a joint presentation, focusing on state-of-the-art in the field, today's challenges in both the experimental and numerical approaches, and how the ProNoVi project is addressing those. ProNoVi is funded by the European Union. Further information is available at www.martera.eu/projects/pronovi.

Keywords: Underwater Acoustics, Propeller cavitation, Turbulence, CFD, Ffowcs-Williams Hawkings

1. INTRODUCTION

Ships feature multiple sources of noise, with the machinery typically emitting in the frequency ranges between 1 and 50Hz and the propeller creating peaks in the orders of multiples of its propeller blade frequency between 10 and 200Hz. While the sources of each of these peaks can be identified easily by their frequency, there is an additional broadband noise spectrum typically attributed to propeller induced cavitation. Both of the aforementioned noise sources factor into human health and comfort onboard ships, the main contributor to the underwater noise spectrum is the propeller cavitation. It appears in many applications with high area load and low cavitation numbers, with increasing extent in off-design operation. There are cavitation types which are avoided during propeller design, when they are known to lead to significant noise or erosion on the blade surface, for example pressure side cavitation. Contemporary propeller designs allow for stable suction side sheet and tip vortex cavitation. The underwater noise generation by these cavitation types and secondary effects in combination with the turbulence, structure and rudder are the main focus in this research

[1] jkimmerl@schottel.de
[2] vladimir.krasilnikov@sintef.no
[3] mario.felli@cnr.it
[4] m.abdel-maksoud@tu-harburg.de
[5] nils.reichstein@luerssen.de

project.

The radiated underwater noise due to shipping activities raises the natural underwater background noise level in the frequency range from 10 to 300Hz by an estimated 20 to 30 dB. With an increase of about 3dB per decade, this development is extremely fast in comparison to evolutionary timescales for some of the affected sea fauna to adapt. Low frequency noise covering the 63 Hz to 125 Hz 1/3 octave bands is dominated by propeller cavitation. This frequency band of emission coincides with important frequencies of perception of whales, marine mammals and fish, which can be observed in masking, behavioral responses and physiological stress in the affected specimen (1). These concerns are addressed in EU Commission decisions (2,3) and IMO Guidelines (4), which in turn leads to international regulations pushed by classification societies (5). Besides the noise emissions interfere with acoustic sensors of naval, research and oceanographic vessels and underwater monitoring systems.

The project “Analysis Methods and Design Measures for the Reduction of Noise and Vibration Induced by Marine Propellers” (ProNoVi) aims to deliver reliable tools for predicting different types of propeller cavitation and the dynamics in operation behind a ship hull, to advance hydroacoustic and noise propagation models in this context and to generate practical recommendations for noise mitigation measures regarding both the radiated and on-board noise levels.

2. PROJECT STRATEGY

In previous projects, propeller induced cavitation and the following collapse of cavities are identified as the primary sources of underwater radiated noise. These projects usually focus on either single phenomena as source of underwater noise or are limited to specific parts of ships, particularly the propeller. Due to the complexity of the effects causing underwater noise, these approaches give valuable insight on the underlying physics. In ProNoVi the entire system of ship and propeller and their interaction is considered, in an effort to make the noise prediction technology ready for industry use in a design tool. The output consists of recommendations and guidelines for industry, research and academia, and regulating societies. In order to generate industry relevant expertise, the investigation considers three existing ship and propeller geometries, a twin screw mega yacht with fixed pitch propellers, a 155m single screw container ship with controllable pitch propeller and a 24m twin screw catamaran for servicing wind farms. The first is designated the reference target case, which is examined in two experimental facilities and full-scale, and provides validation for numerical investigations regarding cavitation and noise radiation.

ProNoVi has four interconnected sub-projects that are aiming to advance methods in their respective area beyond the current state of the art. In the “experimental investigations” sub-project, methods to accurately measure noise generation are developed, validation studies for the simulations are conducted, fundamental mechanisms of propeller cavitation and noise generation are analyzed, and the noise reduction measures found in the other work packages are validated in two model test facilities, SINTEF Ocean (SO) and National Research Council - Institute of Marine Engineering (INM). In the “flow simulation models” sub-project SO, SCHOTTEL, and Lürssen numerically analyze the target cases and identify noise mitigation measures. To reach this objective, the propeller is simulated in open water and behind ship condition for various loadings and cavitation numbers in model and full-scale, mirroring the model tests. The quantification of full-scale effects on propeller generated noise with numerical methods is an additional area of interest within the project. Tools for the numerical investigations are StarCCM+ and OpenFOAM. Examined aspects are turbulence and cavitation models, grid and time step refinement, interface influence by sliding mesh and overset grid, adaptive mesh refinement and modification of conservation equations to reduce numerical diffusion. The sub-project “design oriented tools” deal with the improvement of the acoustic prediction with a boundary element method (BEM) called *pan*MARE developed by Technical University Hamburg-Harburg. Using the validation data from experiments and simulations, the cavitation model is extended. “Noise reduction measures” are extracted during the project runtime from all findings, and in parallel developed and examined with the flow simulation models and design oriented tools.

3. EXPERIMENTAL METHODS

3.1 Model-scale Data

There are few test cases with 3D data of propeller cavitation, thus validation of numerical methods

is often sought in visually comparing cavitation tunnel photographs. The experimental methods employed in ProNoVi are aimed at providing high quality model scale experimental data to go in-depth into the fundamental underlying mechanisms of noise generation and propagation, and at validating the computational tools for cavitation and noise prediction. To this end, standard methodologies for propeller wake flow, cavitation and underwater radiated noise assessment (i.e. optical techniques, such as PIV and LDV, time resolved visualizations, noise and pressure pulse measurements) are integrated with unconventional approaches including stereometry and advanced velocity-pressure/visualization–pressure conditional techniques (6). The experimental program is conducted in the large free surface cavitation channel of CNR-INM and in the cavitation tunnel of SINTEF OCEAN on a reference propeller model operating in open water at different shaft inclinations and in behind-hull condition, with and without the rudder, under a comprehensive range of operative conditions in terms of propeller loading and cavitation number.

3.2 Full-scale Data

For verification purposes the project uses full-scale measurement data available for the target case. The full-scale data is collected with the vessel passing a hydrophone on a track, as shown in Fig. 1.

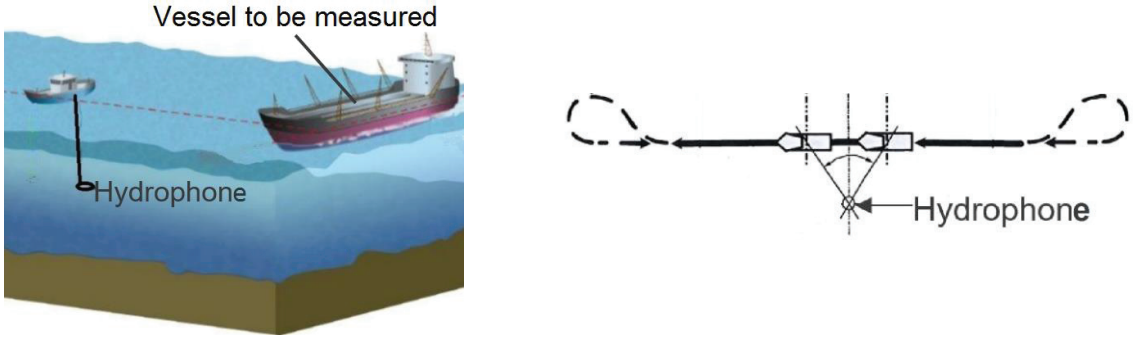

Figure 1 – Full-scale measurement principle (7) and schematic of measurement track (8)

It is represented in a way that the ship is assumed to be a point source. To obtain the sound source level at a normalized distance from the received level, the propagation losses are adjusted

$$SL(f) = RL(f) + TL(f, T_S, T_R, r, D, \alpha), \quad (1)$$

respecting the properties of the source, depth T_S and frequency, and the measurement setup, depth of the hydrophone T_R, horizontal distance r, water depth D and reflection coefficient α. The water depth is measured with the target vessels echo sounder, the hydrophone depth is calculated from the submerged cable length and the angle at the water surface, the distance between ship and hydrophone is calculated from GPS-data, the sea floor properties are taken from a geological map. The results of the measurement are corrected regarding the environment influences and given as monopole source levels according Urban (9), which ensure comparability of measurements under different conditions or with other ships.

4. NUMERICAL METHODS

4.1 Ffowks-Williams Hawkings Equations

There are two types of numerical tools utilized in the project, which are the finite volume method with a certain degree of turbulence modelling (CFD), and a boundary element method as a design tool for iterative propeller und hull design (BEM). While the near-field pressure fluctuations can be evaluated directly by CFD methods on the surfaces adjoining the sound sources, due to the assumption of incompressibility in the applied CFD methods, the solution accuracy decreases in the far-field and considering reflection at the sea floor or free surface is inaccurate. Thus another method for evaluating the far-field noise independently of the flow solution is required.

In aeroacoustics, models that do not require any flow assumptions, which are reducing the sound sources to point emitters, are frequently in use. This generalized theory is called acoustic analogy and can be directly derived from the mass and momentum equations leading to the inhomogeneous wave equation. While the Lighthill acoustic analogy considers sound sources in a free stream, the Curle analogy extends this approach to consider static surfaces with reflection and diffraction. Finally the Ffowks-Williams Hawkings analogy has no such constraints, and can be applied to moving surfaces. The original Ffowks-Williams Hawkings (FWH) formulation (10) distinguishes the acoustic sources

by types, with a monopole associated with thickness p'_T, a dipole for the lifting forces p'_L and a quadrupole for non-linear contributions p'_Q caused for example by cavitation-turbulence interaction

$$p'(\vec{x},t^*) = p'_T(\vec{x},t^*) + p'_L(\vec{x},t^*) + p'_Q(\vec{x},t^*). \tag{2}$$

The first two acoustic pressure disturbances p' are evaluated on the surfaces of the noise source, the latter is computed as a volume integral. Evaluating the spectrum for high frequencies in this formulation requires excessive storage, as the whole solution field has to be saved for very small time steps, which is conflicting with the goal of investigating the broadband noise appearing in high frequency ranges, caused by propeller induced cavitation. In addition, this method demands high computational effort to solve the volume integral in each time step. Hence, the porous formulation of the FWH equation (11), where the sound sources are evaluated by a surface integral on a control volume around the propeller and its wake, is superior. In turn this necessitates a high mesh resolution within the control surface to eliminate dispersion and dissipation errors. In this formulation the terms lose their original physical meaning and p'_T is called pseudo-thickness and p'_L pseudo-loading (12). Assuming the control surface surrounds all non-linear sources, which is valid if the length encompasses the full turbulent wake, their contribution $p'_Q(\vec{x},t) \to 0$ and is thus included in the surface integral. As the ship's hull itself is another source, the location of the control surface is a critical aspect of ProNoVi. For both BEM, as in house implementation, and CFD, for OpenFOAM from the libAcoustics library (13), the Farassat 1A formulation (14), with the time derivatives as an input into the surface integrals, is utilized

$$p'_T(\vec{x},t^*) = \frac{1}{4\pi}\int_S \left[\frac{\rho_0(\dot{v}_n+v_{\dot{n}})}{r(1-M_r)^2}\right]_{ret} dS + \frac{1}{4\pi}\int_S \left[\frac{\rho_0 v_n(r\dot{M}_r+cM_r-cM^2)}{r^2|1-M_r|^3}\right]_{ret} dS, \tag{3}$$

$$p'_L(\vec{x},t^*) = \frac{1}{4\pi c}\int_S \left[\frac{\dot{l}_r}{r(1-M_r)^2}\right]_{ret} dS + \frac{1}{4\pi}\int_S \left[\frac{l_r-l_M}{r^2(1-M_r)^2}\right]_{ret} dS + \frac{1}{4\pi c}\int_S \left[\frac{l_{r(r\dot{M}_r+cM_r-cM^2)}}{r^2|1-M_r|^3}\right]_{ret} dS. \tag{4}$$

Here ρ_0 is density of the fluid, $\vec{v}$ the relative velocity, $\vec{r}$ the distance from the sound source to the observer point $\vec{x}$, M the Mach number, S the body surface and $\vec{l} = p\vec{n}$ the pressure in surface unit normal direction $\vec{n}$. The subscripts represent a dot product of the vector with the unit normal vector $\vec{n}$ on the surface into the fluid, its time derivative $\dot{\vec{n}}$, the unit radiation vector $\hat{\vec{r}}$ or the surface velocity Mach number vector $\vec{M}$. Integrands with r^{-1} can be considered far-field and with r^{-2} near-field terms. With the sound sources on the control volume, the far-field sound pressure is known for arbitrary points, not confined to the initial simulation domain, and at all times within the simulation time range, by interpolation between adjacent time steps.

Due to the sound velocity, the values on the control surface are generated from the time of emission, by linearly interpolating the locations of surfaces at the retarded time between two adjacent time steps $t_1 \le t_{ret} \le t_2$ considering the distance from source to observer

$$t_{ret} = t^* - \frac{||\vec{x}(t^*)-\vec{y}(t)||}{c}, \tag{5}$$

with $\vec{y}$ as the sound source point.

Except for the cavitation tunnel test simulations, reflection modelling is neglected within the CFD methods, due to the size of the domain. It is a very important factor in determining the influence of the experimental facility and compare with the full-scale measurements. A comparison regarding reflection at surfaces is shown in the non-cavitating propeller induced pressure field calculated with *pan*MARE in Fig. 2. Although it is not included in the flow simulation, reflection is modelled in the solution of the FWH equation by mirroring the sources at the reflection surfaces, taking into account the acoustic properties of both materials at the interface. This results in a correction with a reflection factor R, ranging between 0 for no reflection and 1 for full deflection, and pressure p'_Γ on the sum of pressures (15)

$$R = \frac{m\cos^2\Theta - n\sqrt{1-\frac{\sin^2\Theta}{n^2}}}{m\cos^2\Theta + n\sqrt{1-\frac{\sin^2\Theta}{n^2}}}, \tag{6}$$

$$p'_{sum}(\vec{x},t^*) = p'(\vec{x},t^*) + Rp'_\Gamma(\vec{x},t^*), \tag{7}$$

with $m = \frac{\rho_1}{\rho}$ and $n = \frac{c}{c_1}$ and the incident angle Θ. On the boundaries to materials more dense than water the root term in Eq. 6 becomes negative, so reference values from the literature are utilized to model measurement conditions (16).

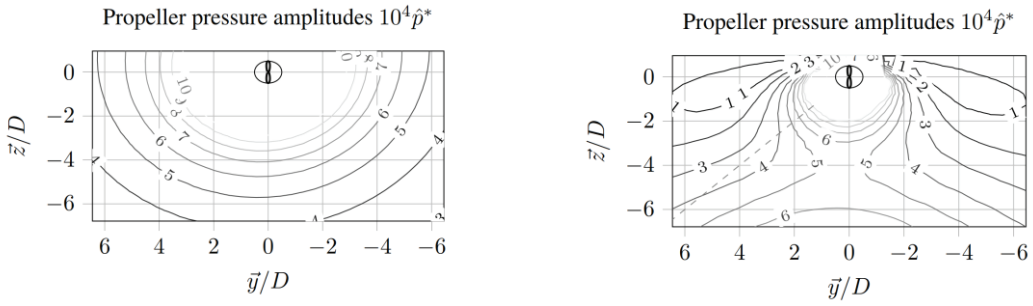

Figure 2 - Comparison of normalized pressure amplitudes of the non-cavitating propeller and hull with (right) and without (left) reflections at the free surface and the sea floor

4.2 Frequency Domain Evaluation

The time domain results at the specified measurement points from the model and full-scale measurements are converted to a frequency domain spectrum with a fast Fourier transform. To reduce spectral leakage, a Hahn window is using integer multiples of the most significant period in the time domain, which typically means the propeller blade frequency. The pressure amplitudes in the frequency domain are then converted to sound pressure levels with the reference pressure identical to the full-scale measurements of $p_{ref} = 1\,\mu Pa$

$$SPL = 10\log\left(\frac{p'}{p_{ref}}\right)^2. \tag{8}$$

4.3 Computational Fluid Dynamics

4.3.1 Turbulence modelling

For the scale-resolved turbulent finite volume investigations, the implicit large eddy simulation (ILES) in OpenFOAM and improved delayed detached eddy simulation (IDDES) in StarCCM+ are chosen, as they promise the best results with the least computational effort, such that they are still possible to be applied in the industry in certain cases. Deducting from previous works by other authors (17) and simulations with a simple twisted hydrofoil shown in Fig. 3, the quality of the resolution of turbulence regarding sheet cavitation in an ILES appears adequate for ProNoVi.

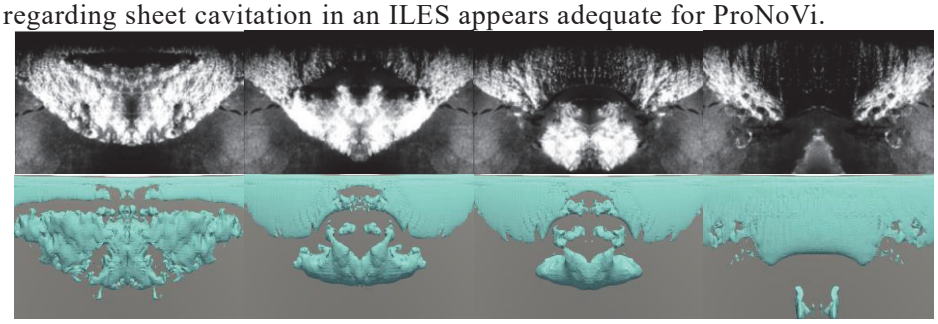

Figure 3 - Comparison experiment (18) and ILES of sheet cavitation pattern over Delft Twist11 Foil

Both CFD approaches rely on the mass and momentum equations to resolve the flow field up to a turbulence scale defined by a filter function $G = G(\vec{x}, \Delta)$

$$\partial_t \rho + \nabla \cdot \left(\rho \bar{\vec{v}}\right) = 0, \tag{9}$$

$$\partial_t \left(\rho \bar{\vec{v}}\right) + \nabla \cdot \left(\rho \bar{\vec{v}} \otimes \bar{\vec{v}}\right) = -\nabla \bar{p} + \nabla \cdot (\bar{\boldsymbol{S}} - \boldsymbol{B}). \tag{10}$$

In this derivation (19), which neglects commutation errors, filtered variables are shown by the overbar and $\boldsymbol{S} = \boldsymbol{2\mu D}$ is the viscous stress tensor with the strain rate tensor $D = \frac{1}{2}(\nabla\vec{v} + \nabla\vec{v}^T)$ and the dynamic viscosity μ. In the unresolved transport term $\nabla \cdot \boldsymbol{B}$ the subgrid stress tensor is introduced (20)

$$\boldsymbol{B} = \rho\left(\overline{\vec{\vec{v}} \otimes \vec{\vec{v}}} - \bar{\vec{\vec{v}}} \otimes \bar{\vec{\vec{v}}} + \widetilde{\boldsymbol{B}}\right). \tag{11}$$

The ILES approach requires no subgrid viscosity to model the remaining $\widetilde{\mathbf{B}}$ as the dissipative qualities can be mirrored by the truncation error τ of the convective terms (21). In ProNoVi the impact of different discretization approaches on the numerical diffusion are investigated. The

linear-upwind stabilized transport scheme (LUST), which combines the error of the central differencing (CDS) and linear upwind differencing scheme (LUDS) $\tau_{LUST} = 0.75\tau_{CDS} + 0.25\tau_{LUDS}$, promising good results in accordance with the correct high wavenumber damping yielding the -5/3 slope of the logarithmic Kolmogorov turbulence energy spectrum in the inertial subrange.

For IDDES the values below the filtered scale are modelled using the RANS k-ω-SST turbulence model with All Y+ Treatment algorithm at solid boundaries. The DDES method introduces a delay factor that enhances the ability of the model to distinguish between LES and RANS regions on meshes where spatial refinement could lead to ambiguous behavior. Further, in the improved (IDDES) formulation, the sub-grid length-scale includes a dependence on the wall distance. This approach allows RANS to be used in a much thinner near-wall region, thus providing some wall-modelled LES capabilities. A hybrid 2nd-order upwind/bounded-CDS is used for modelling the convection terms. Validation cases studied in ProNoVi, for example Fig. 4 (left), show that the present IDDES method yields stable solution through the range of propeller loadings, in both non-cavitating and cavitating cases, and the predicted propeller forces are close to the results obtained with the RANS method.

4.3.2 Vorticity confinement

To counter numerical diffusion in the tip vortex due to the convective term in OpenFOAM, the adaptive vorticity confinement method (VC) artificially convects vorticity back to the vortex center by adding a source term S on the right hand side of the incompressible momentum equation (22)

$$\vec{S} = \varepsilon\, \vec{s} = \varepsilon \frac{\nabla|\vec{\omega}|}{|\nabla|\vec{\omega}||} \times \vec{\omega}. \tag{12}$$

In its original formulation the user has to define a proportionality factor ε to control the strength of the source term, influencing a vectorial quantity along the vorticity $\vec{\omega}$ magnitude contour lines, which necessitates a calibration. To circumvent this, the adjusted model (23) estimates the factor by approximating the diffusive error $\vec{D}$ between the CDS and LUST scheme

$$\varepsilon = \frac{1}{|\vec{s}|^2} \vec{D} \cdot \vec{s}. \tag{13}$$

The approximation is $\vec{D} \approx [(\vec{u} \cdot \nabla)\vec{u}]^{CDS} - [(\vec{u} \cdot \nabla)\vec{u}]^{LUST}$ and the absolute value of ε has to be entered into Eq. 12, as unphysical sign changes may appear near the vortex core. The method is implemented in OpenFOAM (24) and comparison with RANS calculations, in Fig. 4 (right) for a hydrofoil test case (25), confirm the applicability in ProNoVi.

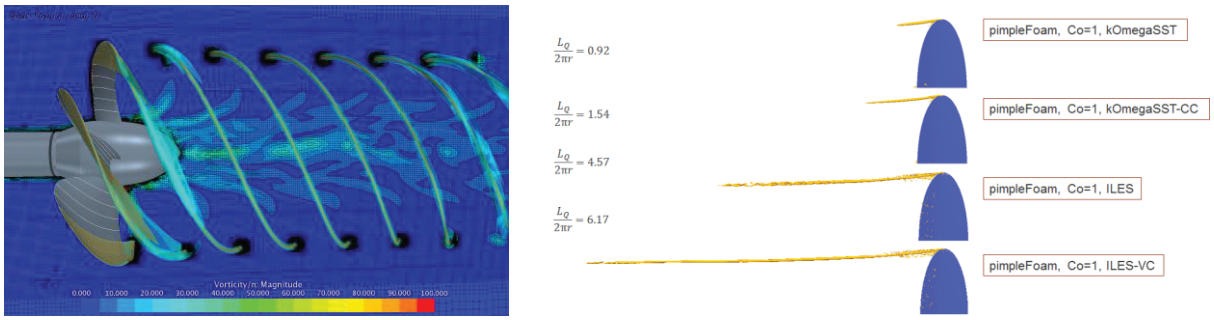

Figure 4 - PPTC propeller case (left), vorticity magnitude and resolved tip vortex: hydrofoil case (right)

In Star-CCM+ an extended rotating region (Sliding Mesh) around the propeller in combination with Adaptive Mesh Refinement (AMR) is used instead of VC method, to counter the effect of numerical diffusion. In the presence of a rudder, an Overset Mesh method is investigated, to extend the rotating region over the rudder in an effort to reduce diffusion at the mesh interface. In preliminary propeller open water tests with the AMR method it is found that the cell size in the tip vortex area needs to be as fine as 0.125% of the propeller diameter in non-cavitating cases, and 0.06-0.08% in cavitating cases.

4.3.3 Phase-Change

To model cavitation the volume of fluid (VOF) method is selected, as it is still computationally feasible and is not oversimplifying. As the two phases are resolved on an Eulerian grid, the fluid interfaces are reconstructed depending on the phase contents in boundary cells. With the exact value unclear this is a topic of discussion, as it is expected that the resulting cavity size has significant impact on noise generation. In tested cases the Full Cavitation Model by Singhal (26) as implemented in OpenFOAM proves numerically unstable and in need of additional calibration. The Full Rayleigh-Plesset cavitation model implemented in Star-CCM+ (27), which is based on the classical (non-simplified) Rayleigh–Plesset equation, is also tested with the PPTC propeller case. It is found

quite sensitive to the solution state at the moment when the model is enforced, and it requires a very small time step. For these reasons, the asymptotic Schnerr-Sauer cavitation model (28) is presently selected for the studies in ProNoVi, which is independent of empirical values. The applicability to sound source modelling is validated by other authors (9) and in the simulations shown in Fig. 3. An additional scalar transport equation is solved for the volume fractions of the phases with an equivalent mass transfer rate of

$$\dot{m} = C\frac{\rho_l\rho_v}{\rho}(1-\alpha)\alpha\frac{3}{R}\sqrt{\frac{\frac{2}{3}(p-p_v)}{\rho_l}}\ , \tag{14}$$

where R depends on the water quality properties, nuclei density and mean nuclei radius. In the derivation from the Rayleigh-Plesset equation, the effects of surface tension, viscosity and thermodynamics are neglected and higher order terms are ignored.

4.4 Boundary Element Method

The BEM approach is based on the assumption of irrotational, incompressible and inviscid flow with the governing equations reducing to the Laplace equation for the velocity potential Φ and the Bernoulli equation for the pressure p (29)

$$\Delta\Phi = \nabla^2\Phi = 0, \tag{15}$$

$$p + \rho g z + \frac{1}{2}\rho(\nabla\Phi)^2 + \frac{\partial\Phi}{\partial t} = const. \tag{16}$$

Applying the Green identity with an impermeability condition on the body boundaries and the cavity surfaces and taking into account the Kutta boundary condition at the trailing edge to create the force-free propeller wake, a unique solution to Eq. 15 is found (30). The cavity surfaces are calculated iteratively with an additional dynamic boundary condition requiring the vapor pressure p_v on the surface. *pan*MARE is solving this boundary value problem numerically with a low order panel-method on quadrilateral panels with constant monopole and dipole strengths on the panels (16). From this results a velocity distribution and the corresponding pressure distribution from Eq. 16.

5. OUTLOOK

Practically, the results of ProNoVi improve compliance of ships and propeller designs with regulations, reduce impacts on the environment, and improve safety and comfort on board ships. The findings serve for elaboration of regulations and guidelines developed by classification societies. The methods developed, facilitate the evaluation of design concepts and troubleshooting of existing designs. For ship operators it results in long-term economic advantages, as compliance with international regulations can be achieved with efficient mechanisms and renovation costs can be reduced. Scientifically the projects results have high value in ship hydrodynamics, numerical modelling of full-scale ship flows, flow unsteadiness, turbulence, cavitation and hydroacoustics. Subsequent research can be expected considering incompressibility effects, interface capturing of the mixture and possibly energy transfer in cavitation processes.

ACKNOWLEDGEMENTS

The authors are very grateful for the support and funding by MarTERA, represented by BMWi-project (03SX461C) “ProNoVi” for the German partners, the Research Council of Norway for the Norwegian Partners (Project 284501) and MIUR-project “ProNoVi” for the CNR-INM.

REFERENCES

1. Merchant N. Impacts of underwater noise on marine resources. In: QUIETING SHIPS TO PROTECT THE MARINE ENVIRONMENT: Technical Workshop. London; 2019.
2. EU. Commission Decision 2010/477/EU. 2010;
3. EU. Commission Decision 2017/848/EU. 2017;
4. IMO. Guidelines for the Reduction of Underwater Noise from Commercial Shipping to Address Adverse Impacts on Marine Life. 2014.
5. DNV-GL. Silent Class Notation. 2010.
6. Felli M, Grizzi S, Falchi M. A novel approach for the isolation of the sound and pseudo-sound contributions from near-field pressure fluctuation measurements: analysis of the hydroacoustic and

hydrodynamic perturbation in a propeller-rudder system. Experiments in Fluids. 2014;55–1(1651).
7. Robinson SP, Hazelwood RA. Good Practice Guide for Underwater Noise Measurement. In: NPL Good Practice Guide. National Measurement Office, Marine Scotland, The Crown Estate; 2014.
8. ISO/TC 43/SC 3. ISO 17208-1:2016 Underwater acoustics -- Quantities and procedures for description and measurement of underwater sound from ships -- Part 1: Requirements for precision measurements in deep water used for comparison purposes. ISO; 2016.
9. Urban H. Handbuch der Wasserschalltechnik. STN Atlas Elektronik GmbH; 2002.
10. Ffowcs Williams JE, Hawkings DL. Sound generated by turbulence and surfaces in arbitrary motion. Philosophical Transactions of the Royal Society. 1969;321–42.
11. Di Francescantonio P. A new boundary integral formulation for the prediction of sound radiation. Journal of Sound and Vibration. 1997;491–509.
12. Lidtke AK, Turnock SR, Humphrey VF. Characterisation of sheet cavity noise of a hydrofoil using the Ffowcs Williams-Hawkings acoustic analogy. Computers & Fluids. 2016;8–23.
13. Korchagova V, Kraposhin M, Strijhak S. Computational Aeroacoustics Methods with OpenFOAM v. 4.1. In: 12th OpenFOAM Workshop. Exeter, England; 2017.
14. Brentner KS, Farassat F. Modeling aerodynamically generated sound of helicopter rotors. Progress in Aerospace Sciences. 2003;83–120.
15. Mei CC. Wave propagation, Chapter three, Two dimensional waves [Internet]. 2004 [cited 2019 May 11]. Available from: http://web.mit.edu/1.138j/www/material/chap-3.pdf
16. Göttsche U, Scharf M, Berger S, Abdel-Maksoud M. A Hybrid Numerical Method for Investigating Underwater Sound Propagation of Cavitating Propellers. In: Fifth International Symposium on Marine Propulsors. Espoo, Finland; 2017.
17. Asnaghi A, Feymark A, Bensow RE. Effect of Turbulence Closure on the Simulation of the Cavitating Flow on the Delft Twist11 Foil. In: 16th Numerical Towing Tank Symposium. Mulheim, Germany; 2013.
18. Foeth EJ, Van Doorne CWH, Van Terwisga T, Wieneke B. Time resolved PIV and flow visualization of 3D sheet cavitation. Experiments in Fluids. 2006;503–13.
19. Sagaut P. Large Eddy Simulation for Incompressible Flows. New York: Springer; 2006.
20. Bensow RE, Fureby C. On the justification and extension of mixed models in LES. Journal of Turbulence. 2007;
21. Bensow RE, Liefvendahl M. Implicit and Explicit Subgrid Modeling in LES Applied to a Marine Propeller. In: 38th Fluid Dynamics Conference and Exhibit. Seattle; 2008.
22. Steinhoff J, Yonghu W, Mersch T, Senge H. Computational vorticity capturing: application to helicopter rotor flow. In: 30th Aerospace Sciences Meeting and Exhibit. 1992.
23. Hahn S, Iaccarino G. Towards adaptive vorticity confinement. In: 47th AIAA Aerospace Sciences Meeting including The New Horizons Forum and Aerospace Exposition. Orlando, USA; 2009.
24. Feder DF, Dhone M, Kornev N, Abdel-Maksoud M. Comparison of different approaches tracking a wing-tip vortex. Ocean Engineering. 2018;659–75.
25. Arndt REA, Arakeri VH, Higuchi H. Some observations of tip-vortex cavitation. Journal of fluid mechanics. 1991;269–89.
26. Singhal AK, Athavale MM, Li H, Jiang Y. Mathematical Basis and Validation of the Full Cavitation Model. Journal of Fluids Engineering. 2002;617–24.
27. Muzaferija S, Papoulias D, Peric M. VOF Simulations Of Hydrodynamic Cavitation Using The Asymptotic And Classical Rayleigh-Plesset Models. In: Fifth International Symposium on Marine Propulsors. Espoo, Finland; 2015.
28. Sauer J, Schnerr GH. Development of a new cavitation model based on bubble dynamics. Zeitschrift für Angewandte Mathematik und Mechanik. 2001;561–2.
29. Katz J, Plotkin A. Low-Speed Aerodynamics. Cambridge, UK: Cambridge University Press; 2001.
30. Berger S, Bauer M, Druckenbrod M, Abdel-Maksoud M. Investigation of Scale Effects on Propeller-Induced Pressure Fluctuations by a Viscous/Inviscid Coupling Approach. In: Third International Symposium on Marine Propulsors. Launceston, Australia; 2013.